Bioresource Technology 138 (2013) 30–37

Contents lists available at SciVerse ScienceDirect

Bioresource Technology

journal homepage: www.elsevier.com/locate/biortech

Evaluation of intracellular lipid bodies in *Chlamydomonas reinhardtii* strains by flow cytometry

Natarajan Velmurugan [a,1], Minji Sung [a,1], Sung Sun Yim [a], Min S. Park [a,b,*], Ji Won Yang [a,*], Ki Jun Jeong [a,*]

[a] Department of Chemical and Biomolecular Engineering, KAIST, Yuseong-gu, Daejeon 305-701, Republic of Korea
[b] Bioscience Division, Los Alamos National Laboratory, Los Alamos, NM, USA

HIGHLIGHTS

- Optimized FACS condition for single-cell sorting of *C. reinhardtii* and its mutants.
- Comparison of BODIPY 505/515 and NileRed for FACS screening of microalgae.
- Found that BODIPY 505/515 with less concentration of DMSO effective for FACS.
- Distinguished *C. reinhardtii* and its mutants by chlorophyll level with FACS.
- Established a quantitative baseline for lipids accumulation and/or microalgal growth.

ARTICLE INFO

Article history:
Received 7 December 2012
Received in revised form 9 March 2013
Accepted 11 March 2013
Available online 19 March 2013

Keywords:
Lipid
Fluorescence-activated cell sorting
Single cell sorting
Chlamydomonas reinhardtii
BODIPY 505/515

ABSTRACT

A comparative study of *Chlamydomonas reinhardtii* wild type CC124 and a cell wall-less mutant sta6-1 is described using FACS in conjunction with two different lipophilic fluorescent dyes, Nile Red and BODIPY 505/515. The results indicate that BODIPY 505/515 is more effective for the vital staining of intracellular lipid bodies and single cell sorting than Nile Red. While BODIPY 505/515 stained cells continued to grow after single cell sorting using FACS, Nile Red stained cells failed to recover from sorting. In addition, a comprehensive study was performed to establish a quantitative baseline for future studies for either lipid accumulation and/or microalgal growth by measuring various parameters such as cell count, size, fatty acid contents/composition, and optical/confocal images of the wild type and mutant.

1. Introduction

Microalgal biomass has gained substantial support as a potential alternative to petroleum-based transportation fuels through its conversion to various forms of biofuels such as biodiesel and bioethanol (Beer et al., 2009; Williams and Laurens, 2010). Several microalgal species have been screened for the high level production of lipids (Banerjee et al., 2002; Chisti, 2007). In microalgae, lipids synthesized in vivo are classified into two groups, either neutral or polar lipids (Li et al., 2010). The neutral lipids, triacylglycerides (TAG), are energy-rich compounds which can be converted to biodiesels and jet fuels (Goodson et al., 2011; Radakovits et al., 2010).

The green unicellular microalgae *Chlamydomonas reinhardtii* has been used as a model system to study lipid bodies that contain TAG (Goodson et al., 2011; Siaut et al., 2011; Wang et al., 2009). The recent genome sequencing of *C. reinhardtii* makes the species an attractive model for understanding the molecular nature of lipid body formation and TAG synthesis in microalgae (Merchant, 2007; Siaut et al., 2011). Recently, the mechanisms of lipid accumulation in *C. reinhardtii* have been discussed by others (Goodson et al., 2011; Work et al., 2010). Starchless mutants have provided insight into the relationship between starch and lipid accumulation (Siaut et al., 2011). However, there is limited information available on a comparison of lipid accumulation in wild type *C. reinhardtii* and its complementary starchless strain. Thus, it is necessary to conduct a comparative characterization of the growth kinetics, cell size, lipid content and composition under nitrogen replete conditions of these two strains because the majority of earlier reports have been heavily centered on the investigation of the lipid contents of sta6 grown in a N-starved condition (Siaut et al., 2011; Work et al., 2010).

* Corresponding authors. Tel.: +82 42 350 5964; fax: +82 42 350 3910 (M.S. Park), tel.: +82 42 350 3924; fax: +82 42 350 8858 (J.W. Yang), tel.: +82 42 350 3934; fax: +82 42 350 3910 (K.J. Jeong).
E-mail addresses: minsungpark0@kaist.ac.kr (M.S. Park), jwyang@kaist.ac.kr (J.W. Yang), kjjeong@kaist.ac.kr (K.J. Jeong).
[1] These authors equally contributed to this work.

0960-8524/$ - see front matter © 2013 Elsevier Ltd. All rights reserved.
http://dx.doi.org/10.1016/j.biortech.2013.03.078

Flow cytometry enables the analysis of the different features or physiological states of bacteria, fungi, yeast and mammalian cells at the single cell level (Davey and Kell, 1996) and FACS can be also employed for the analysis of microalgae (Hyke et al., 2013). Flow cytometry can distinguish different microalgae by emission of autofluorescence of algal native pigments such as chlorophylls, carotenoids, or phycobilins (Hyke et al., 2013). Flow cytometry, when combined with a suitable fluorescent dye, offers a unique opportunity to rapidly isolate microalgae with high lipid content for the production of biofuels (Cooper et al., 2010). The lipophilic dye Nile Red has been most commonly used to detect microalgal lipids, such as in the work of Doan and Obbard (2011b) where they measured the lipid content in *Nannochloropsis* using flow cytometry and Nile Red. However, the limitations of Nile Red have encouraged the development of an alternative dye that is effective for detecting microalgal lipids. Recently, Cooper et al. (2010) proposed using another lipophilic dye BODIPY 505/515 as a vital stain for detection of intracellular lipid bodies of microalgae and Pereira et al. (2011) provided evidence that they could isolate a few marine microalgae using flow cytometry in combination with BODIPY 505/515.

Flow cytometry is considered to be a promising high-throughput technique for its ability to interrogate living cells at the single-cell level. By using single cell sorting, it is possible to analyze the physiological states of the cells and their expressed gene functions simultaneously by using a combination of various fluorescent dyes (Czechowska et al., 2008). A FACS-sorted single cell with a distinctive property can be used for further study, for example, single cell genomics. Several fluorescent dyes and probes are commercially available, and can be used for cell component-specific labeling (Czechowska et al., 2008; Hyke et al., 2013). As supported by its effective use for a study of genome replication (Czechowska et al., 2008), FACS can be applied to a single cell genomics study of microalgae by analyzing a specific metabolic activity, such as lipid accumulation, at the single cell-level rather than at the microalgal population-level. If single cell genomics can be incorporated with the metabolic activity of an algal cell, it may be possible to metabolically engineer micro-algae for high lipid and biomass production which is essential for high level production of microalgae-based drop-in fuels.

Herein, a complete characterization of the wild type and starchless complement mutants of *C. reinhardtii* with regard to their cell growth and lipid accumulation is presented. Specifically, the relationship between cellular growth, cell size and accumulation and composition of intracellular lipids in wild type CC124 and the starchless mutant sta6-1 was examined. Furthermore, the use of FACS with BODIPY 505/515 dye was tested for the screening, isolation, and culture of a single cell of *C. reinhardtii* CC124 and mutant sta6-1 to ascertain the potential of FACS for single cell genomics and other applications such as high throughput screening of microalgal strains that are metabolically engineered for high lipid production.

2. Methods

2.1. Strains and culturing conditions

C. reinhardtii (Wild type – CC124) (kindly provided by Korea Research Institute of Bioscience and Biotechnology) and *C. reinhardtii* mutant (cc-4348 sta6-1) (purchased from *Chlamydomonas* Resource Center (www.chlamycollection.org), University of Minnesota, USA) were used in this study. Both cells were grown in nitrogen-supplemented Tris Acetate Phosphate Medium (TAP, Gorman and Levine, 1966). Cultures were maintained at 27 °C under a light intensity of 125 μmol/m^2 s with an agitation speed of 120 rpm. Samples for analysis were taken at different intervals, including 0 h (samples were taken immediately after re-suspension). Optical density was measured using a UV spectrophotometer (Beckman-Coulter DU 730 Life Science, CA) and cell counts were measured by hemocytometer. Cell size was assessed using a dynamic particle counter (Beckman-Coulter, Brea, CA) with the assumption that cells are spherical for diameter calculations. Coulter cell counts were verified for representative samples using microscopy.

2.2. Nile Red staining

Nile Red staining of the intracellular lipid bodies of *C. reinhardtii* was done as reported by Doan and Obbard (2011a). Glycerol (Sigma Aldrich, St. Louis, MO) was added to the microalgae suspension to a final concentration of 0.1 g ml^{-1} and stored in the dark. Five microliters of Nile Red (9-(diethyl amino) benzo[*a*]phenoxazin-5(5*H*)-one, Sigma Aldrich) stock solution (0.4 mg ml^{-1}) was added to 3 ml of the algal-glycerol suspension which was then agitated for 1 min on a vortex mixer. Samples were then incubated in darkness for 5 min at room temperature. After the incubation period, samples were directly used for FACS and microscopic analyses.

2.3. BODIPY staining

BODIPY 505/515 (4,4-difluoro-1,3,5,7-tetramethyl-4-bora-3a,4a-diaza-s-indacen), was purchased from Sigma Aldrich. BODIPY 505/515 staining was performed by a modification of the method described by Cooper et al. (2010). A 5 mM BODIPY 505/515 stock was prepared by dissolving in dimethyl sulfoxide (Sigma Aldrich, St. Louis, MO) and stored in the dark. For efficient staining of the intracellular lipid bodies of *C. reinhardtii*, an aliquot of 0.02–0.2% DMSO (vol/vol) was added to the microalgal suspension. A range of aliquots of BODIPY 505/515 stock solution, from 1 to 10 μM, was added into the algal-DMSO suspension and agitated for 1 min on a vortex mixer. Samples were then incubated in darkness for 5 min at room temperature. After the incubation period, the samples were directly used for FACS and microscopic studies.

2.4. Flow cytometric analysis and cell sorting

A high speed flow cytometer, MoFlo XDP (Beckman Coulter, Fullerton, CA) was used for the analysis of cell staining and cell sorting. The fluorescence reading was obtained using an excitation of 488 nm with an argon laser. The emission signal was measured in three channels upon excitation (FL1 channel centered at 530/40 nm, FL2 channel centered at 580/30 nm (indicative of neutral lipids of Nile Red stained cells), FL3 channel centered at 630/30 nm (indicative of polar lipids of Nile Red stained cells), and FL5 channel centered at 740 LP). The samples mean fluorescence intensity values and images were analyzed using SUMMIT Software Version 5.2. The FACS settings of all channels were the same for all sorting procedures. Coulter Isoton II Diluent fluid (Beckman Coulter, Bera, CA) was used in all experiments as the flow cytometry sheath fluid. Single cell sorting was carried out using the single cell sort precision mode, with a 70 μm nozzle. Single cells were sorted directly into the wells of a deep-96-well plate containing 1 ml of nitrogen-supplemented TAP broth. After cell sorting, plates were incubated for 7–10 days in a shaking rotator under the same growth conditions as described above. Single cell growth was monitored every day and cultures were maintained until the visible healthy algal growth was achieved from a single sorted cell. In order to assess the growth stability of a sorted single cell and the contamination rate, 100 μl of a liquid portion from the wells was spread on a nitrogen-supplemented TAP agar plate and incubated for 7 days under photo intensity of 125 μmol/m^2 s.

2.5. Microscopic determination of lipids in microalgal cells using different fluorescent dyes

A fluorescence microscope, Leica DM2500 (Fluorescence lamp – ebq 100-04), was used to measure the fluorescence intensity of Nile Red and BODIPY 505/515 stained cells. A laser scanning confocal microscope (Eclipse C1si, Nikon, Kanagawa, Japan) with the excitation set at 488 nm and the emission set at 570–590 nm was used for selectively detecting microalgal lipid bodies.

2.6. Total lipid and fatty acid analysis

The total lipids were extracted from the 10 mg of lyophilized biomass with a chloroform–methanol (2:1 v/v) solvent mixture using a procedure similar to Folch's method (Folch et al., 1957). Fatty acid methyl esters (FAMEs) were produced from the extracted lipid by a transesterification reaction. Briefly, methanol was added to the extracted lipids with sulfuric acid as a catalyst and the transesterification reaction was allowed to occur at 100 °C for 10 min. After the reaction, 1 ml of deionized water was added and the organic phase was separated from the water phase by centrifugation at 4000 rpm for 10 min. One ml of chloroform containing 0.5 mg of hepatdecanoic acid (C17:0) (Sigma Aldrich, St. Louis, MO) was added to each tube as an internal standard. The FAMEs in the organic phase were analyzed by gas chromatography (HP5890, Agilent) with a flame ionized detector (FID) and INNOWAX capillary column (Agilent, USA, 30 m × 0.32 mm × 0.5 μm).

2.7. Statistical analysis

Triplicates of samples were analyzed throughout the experiments. Statistical analyses were performed using SigmaPlot 10.0 software. The results were expressed as means of triplicate experiments. The results expressed as means ± SD (standard deviation), are available in the Supplementary information. Differences were considered significant at $p < 0.05$.

3. Results and discussion

3.1. Physiological behavior and morphological features of wild type and the starchless mutant

To obtain healthy growth of *C. reinhardtii* wild type CC124 and the starchless mutant sta6-1, the seed cultures of wild type CC124 and mutant sta6-1 were obtained from late log phase in nitrogen supplemented TAP medium. The initial inoculations of seeds for working cultures were maintained around $\sim 2.0 \times 10^6$ cells ml^{-1}. The growth rates and cell sizes of wild type CC124 and starchless mutant sta6-1 in the presence of nitrogen supplementation were measured and are shown in SI. F.1 and Table 1. Both strains had a similar growth pattern in which they reached the stationary phase by 72 h. The wild type CC124 was found to have a longer stationary phase that lasted from 72 to 120 h than the mutant sta6-1. The mutant sta6-1 showed exponential growth from 24 to 72 h with a gradual decline in cell growth after this time frame (SI. F.1). In the nitrogen supplemented condition, the highest cell growth was found for the sta6-1 mutant than the wild type CC124. In comparison, Work et al. (2010) reported higher cell concentrations for the sta6 mutant compared with the wild type CC124 in the presence of nitrogen-replete TAP medium. It is interesting to observe that the mutant strain grows better than the wild-type regardless of whether nitrogen is present or not. The overall amounts of cell growth for both CC124 and sta6-1 are similar to that observed by Work et al. (2010). The mutant sta6-1 had a smaller average cell size (4.8 μm) than wild type (6.5 μm) perhaps because the sta6-1 mutant phenotype may be related to the cell division rate in TAP medium. However, in the nitrogen supplemented condition, the average cell size of the mutant sta6-1 (4.8 μm) was less than the 5.6 μm reported by Work et al. (2010). However, Work et al. (2010) reported a large cell size (6 μm) for sta6 under a nitrogen depletion condition. This is consistent with the general observation that cell size increases under nitrogen depletion due to a reduced rate of cell division. The wild type CC124 cell diameter is constantly increased from the exponential phase (48 h) to the late-stationary phase (120 h) (Table 1). The final cell size was 6.5 μm, obtained for the wild type under the nitrogen supplemented condition while Work et al. (2010) documented a cell size of 7.2 μm for wild type CC124 under the nitrogen depletion condition. The differences in cell size may be due to differences in the intensity of the photo illumination, pH and rotation speed of orbital shaker between the two experiments. However, it should be noted that in line with the report of Work et al. (2010), the increase in the average cell size fits well the hypothesis of stacked cell division (SI. F.1 and Table 1). The cell sizes were measured using a dynamic particle counter (Beckman-Coulter) that operates on the assumption that the cells in fluid are spherical. The microscopic observations confirmed that sta6-1 cells are perfectly spherical while CC124 cells are somewhat less spherical hence the particle counter should have provided a good approximation of cell size.

Table 1
Average cell sizes of CC124 and sta6-1 cells cultured in TAP medium at different cell growth phases.

Growth phase	Cell diameter[a] (μm)	
	CC124	sta6-1
Exponential phase (48 h)	5.7 ± 0.9	4.7 ± 0.8
Early-stationary phase (72 h)	5.7 ± 1.21	4.7 ± 0.8
Mid-stationary phase (96 h)	6.3 ± 0.7	4.8 ± 0.7
Late-stationary phase (120 h)	6.5 ± 0.4	4.8 ± 0.8

[a] All data are expressed as mean of triplicate experiments.

3.2. Comparison of the lipid content of wild type and the starchless mutant by BODIPY 505/515 and Nile Red staining

One of the aims of this study was to compare the effectiveness of Nile Red and BODIPY 505/515 dyes to stain intracellular lipid bodies of *C. reinhardtii* for flow cytometry-based screening and single cell sorting. During the preparation of this paper, Govender et al. (2012) reported the effectiveness of Nile Red and BODIPY 505/515 as lipid dyes for *Chlorella vulgaris*, *Dunaliella primolecta* and *Chaetoceros calcitrans*. While the results regarding the Nile Red and BODIPY staining of *C. reinhardtii* reported herein were consistent with the results reported by Govender et al. (2012), we also studied the physiological behavior and intracellular lipid accumulation during the cell growth cycle, in combination with fluorescent activated cell sorting to screen and isolate a single *C. reinhardtii* cell possessing high lipid content. Both Nile Red and BODIPY 505/515 are lipophilic fluorescent dyes that have been used for the measurement of intracellular neutral lipids in microalgal cells (Cooper et al., 2010; Doan and Obbard, 2011a). The intake mechanism of both Nile Red and BODIPY 505/515 within an algal cell is well known. Glycerol and/or DMSO are used as a carrier(s) for Nile Red penetration across the cell membrane, and the yellow-gold fluorescence represents intracellular lipid droplets (Doan and Obbard, 2011a). While intracellular lipid droplets adsorb BODIPY 505/515 via a diffusion trap mechanism (Cooper et al., 2010), intake of Nile Red dye within the algal cell varies

among the algal species due to rigidity, structure and thickness of the cell wall (Chen et al., 2009; Cooper et al., 2010).

Several groups have used a Nile Red solution made with different carrier solvents including acetone (Cooksey et al., 1987), glycerol (Doan and Obbard, 2011a) and DMSO (Chen et al., 2009; Doan and Obbard, 2011a). Although acetone and DMSO appear to be good carriers for Nile Red, it is reported that higher quantities of acetone and DMSO inhibit algal cell growth (Doan and Obbard, 2011a). The cell viability is an important point to be considered since one of the major aims of our study was to sort single algal cells with high lipid content and recover those cells for further cultivation. The glycerol-based Nile Red staining method was efficient for these studies.

Fluorescence microscopy images of Nile Red stained wild type CC-124 and mutant sta6-1 are shown in SI. F.2 (b-1 and b-2, respectively). In addition to neutral lipid, Nile Red also stains the polar lipid which emits reddish fluorescence. SI. F.2 shown cells at the stationary phase and we could not find the reddish fluorescent granule of polar lipids. It was already reported that the membrane bound polar lipids began to degrade at stationary phase in *C. reinhardtii* (Goodson et al., 2011; Wang et al., 2009). This might be possible reason that polar lipids were not recognized in the microscopy images. It is seen clearly that glycerol efficiently assisted Nile Red to penetrate the cell wall of *C. reinhardtii* and bind to lipid bodies emitting a yellow fluorescence. Based on this information, the cells were treated with glycerol for further sample preparations for FACS analysis and sorting.

DMSO was used as a carrier molecule for BODIPY 505/515 at a significantly lower final concentration of 0.02–0.2% than previously reported (Chen et al., 2009). The results demonstrated that low concentrations of DMSO (0.02–0.2%) were effective to deliver BODIPY 505/515 into the cell, while BODIPY 505/515 staining in a glycerol-algal suspension was not effective to stain lipid bodies for microscopic and FACS analysis (data not shown). Also, it was determined that these significantly lower concentrations of DMSO were not toxic to single cell of *C. reinhardtii* and maintained the suitability of the system for single cell sorting and further recovery of independent cultures. The lipid bodies of BODIPY 505/515 stained *C. reinhardtii* were clearly distinguished from chloroplasts and other intracellular organelles by their emission of green fluorescence (SI. F.2 and SI. F.3). Very clear bright green lipid droplets of *C. reinhardtii* CC124 were observed in both confocal and fluorescence microscopy images and BODIPY 505/515 did not bind to other cytoplasmic components other than lipid bodies (SI. F.2 and SI. F.3) (Cooper et al., 2010). BODIPY 505/515 staining of intracellular lipid bodies of CC124 was visualized similarly by both confocal microscope and fluorescence microscope. Cooper et al. (2010) suggests that the narrow emission spectrum of BODIPY 505/515 makes this dye more suitable for technical applications, such as confocal imaging, where fluorescence contrast enhancement of lipid bodies is critical. Overall, the BODIPY 505/515 staining of intracellular lipid bodies provided a better resolved image than was obtained by Nile Red staining.

3.3. FACS analysis of wild type and the starchless mutant of *C. reinhardtii*

Following the staining experiments with Nile Red and BODIPY 505/515 for microscopic studies of lipid bodies, CC124 and sta6-1 were analyzed by using FACS. All experiments were carried out in triplicate and the statistical information can be found in the Supplementary materials (SI. F.4). Fig. 1 shows the two-dimensional plots of auto-fluorescence (a), Nile Red (b), and BODIPY 505/515 (c) stained cells of CC124 and sta6-1. Highly scattered SSC signals were observed for the autofluorescence of CC124 (Fig. 1 a-1). *C. reinhardtii* cells exhibit autofluorescence from endogenous chlorophyll, carotenoid, phycoerythrin, and phycocyanin molecules (Cooper et al., 2010; Pereira et al., 2011). The starchless mutant sta6-1 exhibited a uniform SSC signal (Fig. 1 b-1). A uniform cellular neutral lipid pattern was revealed by two-dimensional plots of the FSC vs. FL2 channel (yellow-gold fluorescence) obtained from the Nile R-

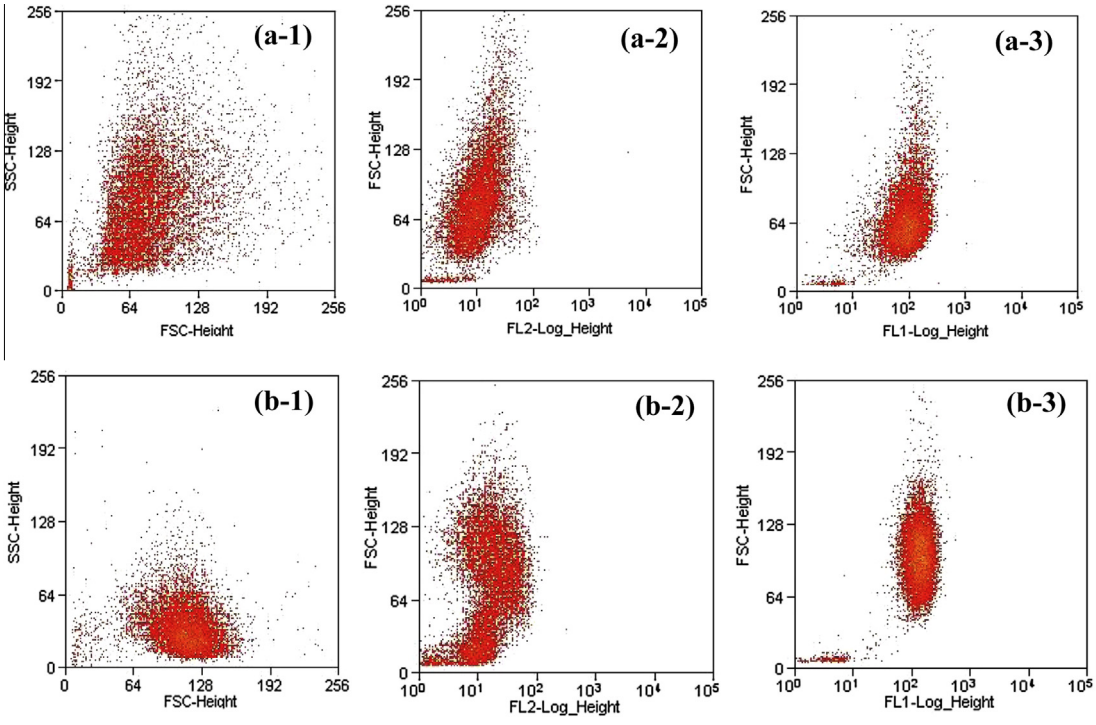

Fig. 1. Two-dimensional dot plots of strains CC124 (a) and sta6-1 (b) for unstained (1), Nile Red (2), and BODIPY 505/515 staining (3).

ed stained cells of CC124 and sta6-1 (Fig. 1 a-2 and b-2), while green fluorescence was detected via the FSC and FL1 channels which were obtained from the BODIPY 505/515 stained cells of CC124 and sta6-1 (Fig. 1 a-3 and b-3). As shown in Fig. 1 (a-2, 3 and b-2, 3), a good separation of signal intensity was obtained for Nile Red and BODIPY 505/515 stained CC124 and sta6-1, indicating the utility of FACS in combination with BODIPY 505/515 for isolation and characterization of microalgal cells for analysis of lipid content and production.

The autofluorescence intensities of sta6-1 in the FL1 and FL2 channels were lower than those in wild type CC124 (blue peaks in Fig. 2). Fig. 2a, b and Table 2 shows the FL2 signals of Nile Red stained CC124 and sta6-1. Nile Red emission maximum can be shifted as the polarity of the medium decreases, which allows one to differentiate between neutral and polar lipids at the excitation and emission wavelengths (Mutanda et al., 2011). In our study, the red fluorescence was detected via FL2 and FL3 channels revealed the neutral and polar lipid contents of Nile Red stained cells, respectively. Even though Nile Red stained both polar lipid and neutral lipid, the fluorescence of each lipid could be distinguished in FACS analysis through the different filer channels (see Section 2). So, the fluorescence of neutral lipid stained with Nile Red could be analyzed independent of polar lipid content. The mean fluorescence intensity of Nile Red in CC124 gradually increased from the exponential to the stationary growth phase (Table 2), indicating the accumulation of neutral lipids. A final fluorescence mean intensity of 47.18 (a.u.) was obtained for CC124 at late-stationary phase (Fig. 2a and Table 2). Cells in exponential phase showed lower mean intensity values, indicating small amounts of lipids in the cells (Table 2). Cells in mid-stationary phase were the most lipid rich (Table 2). However, we unexpectedly observed that the starchless mutant sta6-1 showed a slightly different pattern (a gradual increase as the cells grew) and exhibited significantly lower fluorescence intensity compared with those of wild type CC124 (Table 2). A possible reason for the decrease in signal intensities is that incubation with Nile Red might damage the cell membrane causing membrane leakage. It is reported that the fluorescence capability of Nile Red depends on the polarity and hydrophobicity of the cell (Govender et al., 2012) and Nile Red fluorescence intensity may change when it binds to certain proteins (Cooper et al., 2010), while BODIPY 505/515 does not bind with proteins.

The staining of lipids with BODIPY 505/515 was optimal to 0.2% DMSO as it did not affect cell viability and recovery at this concentration. Unlike the results from Nile Red staining, the mean fluorescent intensity from BODIPY staining of CC124 was the highest in the late stationary phase where it was 89.13 times greater than the autofluorescence (Fig. 2c and Table 2). The mutant sta6-1 attained the highest lipid content in the late stationary phase with a mean fluorescence intensity of 90.50 times greater compared with that of the autofluorescence. Fig. 3 presents a sequence of fluorescence histograms related to the different cell growth phases of CC124 and sta6-1. It is evident that there was a well-defined shift of BODIPY 505/515 from exponential, early-, to late-stationary phases of CC124 and sta6-1 (Fig. 3), indicating the progressive

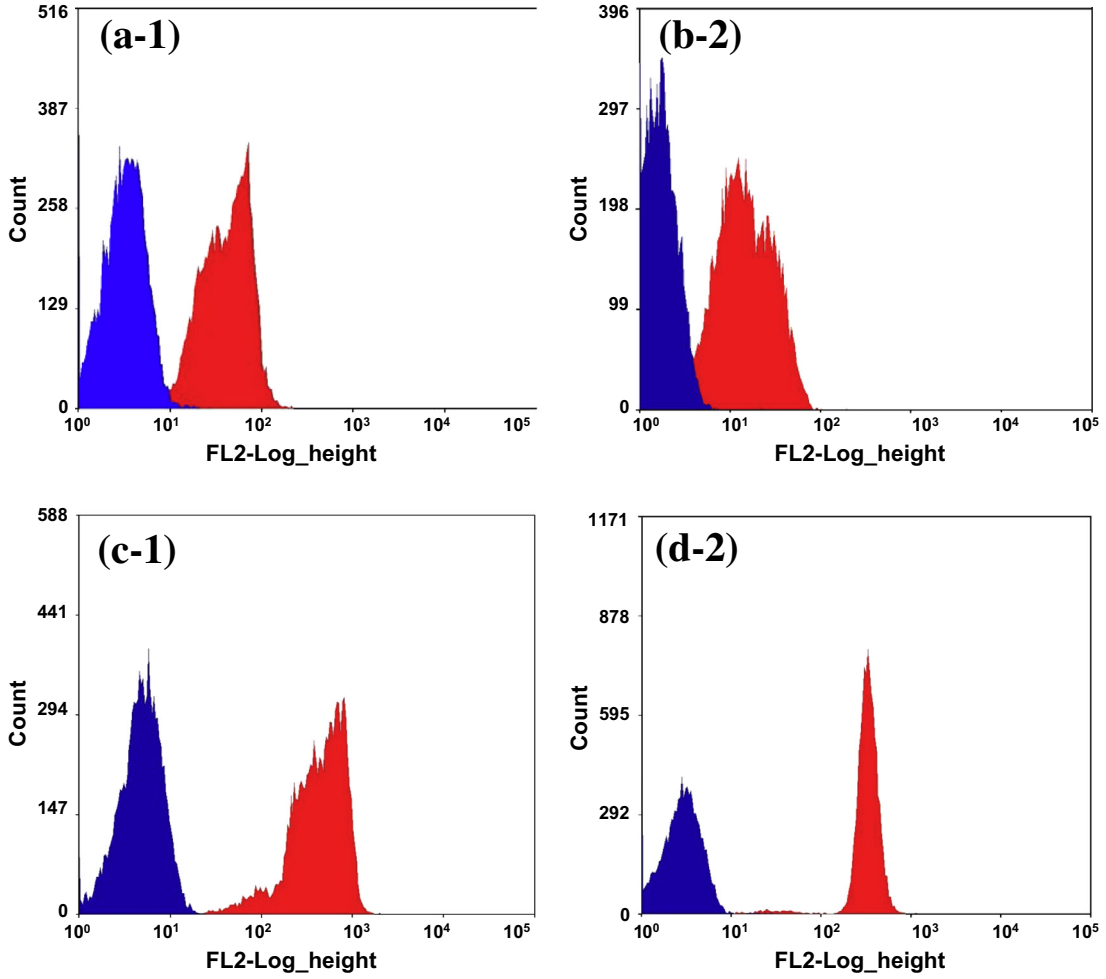

Fig. 2. Flow cytograms of unstained (Blue), Nile Red (Red – a and b), and BODIPY 505/515 (Red – c and d) stained strains of CC124 (1), and sta6-1 (2) at late stationary phase. (For interpretation of the references to colour in this figure legend, the reader is referred to the web version of this article.)

Table 2
Fluorescence intensity of unstained, Nile Red, and BODIPY 505/515 stained strains of CC124 and sta6-1 at different cell growth phases.

Strains and growth phase	Mean fluorescence intensity[a] (a.u.)						
	Unstained FL2[b]	Nile Red stained FL2	Mean fold difference (FL2/FL2[b])	Unstained FL1[b]	BODIPY stained FL1	Mean fold difference (FL1/FL1[b])	FL5
CC124							
Exponential phase (48 h)	3.06	25.52	8.33	5.02	434.54	86.50	23.15
Mid-stationary phase (96 h)	3.20	49.73	15.54	5.55	487.99	87.87	26.49
Late-stationary phase (120 h)	4.19	47.18	11.25	5.53	492.94	89.13	36.63
Sta6							
Exponential phase (48 h)	1.71	4.41	2.59	2.35	228.08	96.91	11.91
Mid-stationary phase (96 h)	1.87	13.78	7.35	2.63	240.19	91.32	11.81
Late-stationary phase (120 h)	1.84	17.92	9.71	2.82	255.23	90.50	11.76

[a] All data are expressed as mean fluorescence intensity of triplicate experiments.
[b] Unstained.

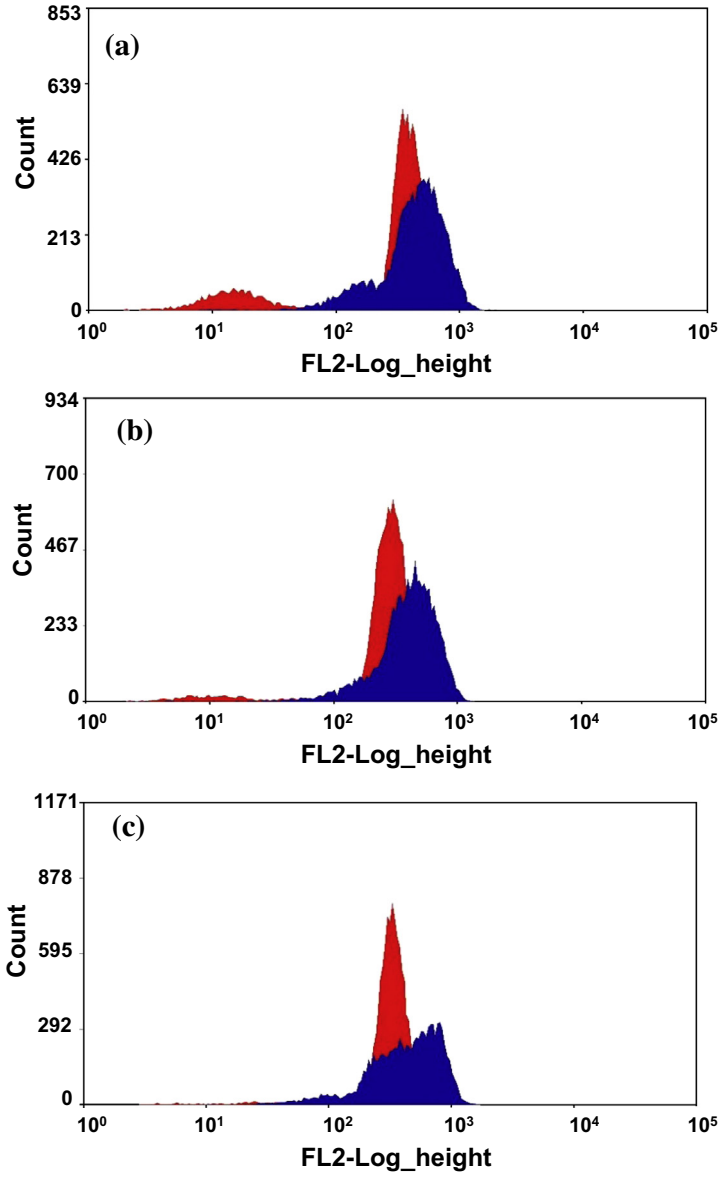

Fig. 3. Flow cytograms of BODIPY 505/515 stained strains of CC124 (Blue), and sta6-1 (Red) at different growth phases, exponential phase (a), early-stationary phase (b), late-stationary phase (c). (For interpretation of the references to colour in this figure legend, the reader is referred to the web version of this article.)

Table 3
GC quantification of FAME content of strains of CC124 and sta6-1 at different cell growth phases.

Strain and growth phases	Total lipid (μg/mg biomass)	Fatty acid (% of total fatty acids)[a]					
		C14:0	C16:0	C16:1	C18:0	C18:1–3 (n)[b]	Other
CC124							
Exponential phase (48 h)	57.03	0.70	37.00	1.73	10.56	29.33	4.36
Mid-stationary phase (96 h)	79.27	0.46	32.63	2.66	8.30	29.43	4.43
Late-stationary phase (120 h)	85.60	0.60	29.60	2.53	4.06	33.63	4.16
Sta-6							
Exponential phase (48 h)	65.47	0.63	40.36	5.40	8.83	27.30	4.96
Mid-stationary phase (96 h)	77.07	0.50	37.66	6.66	5.06	31.73	2.86
Late-stationary phase (120 h)	87.60	0.53	34.33	5.93	3.90	31.43	2.66

[a] All data are expressed as mean quantity of triplicate experiments.
[b] C18:1n9c, C18:2n6t, C18:3n6c.

accumulation of lipids in those cells as the cell cycle moved from the exponential phase to late-stationary phase (Fig. 3).

The FL5 channel was used to effectively distinguish the chloroplast signals from the BODIPY 505/515 green fluorescence (Table 2). Simultaneous measurements of FL1 (green fluorescence) and FL5 (chloroplast fluorescence) were recorded at different growth phases. As shown in Table 2, the chloroplast fluorescence of wild type CC124 at different growth phases was consistently higher than the starchless mutant sta6-1. Therefore, in addition to BODIPY 505/515 staining of lipid bodies, the autofluorescence of the chloroplasts can be used to distinguish the starchless mutant from the wild type.

3.4. Fatty acid composition and quantity of wild type and starchless mutant by GC-FID analysis

To confirm the conclusions drawn from the FACS data, the FAME content of CC124 and sta6-1 at different growth phases (exponential, early-, and late-stationary growth phases) was measured. The statistical information for the triplicate experiments can be found in the Supplementary materials (SI. F.5). In all growth phases, the major fatty acid components observed in CC124 and sta6-1 cells were C16:0, C16:1, C18:0, and C18:1–3 (Table 3). These results are in agreement with recent findings regarding the lipid accumulation in CC124 and sta6 (Work et al., 2010). The overall lipid content observed for CC124 and sta6-1 at different growth phases concur with the FACS data (please refer to the mean fold differences in Table 2 and total lipid content in Table 3). Briefly, lipid contents in early-, and late-stationary phases were significantly increased compared with the exponential phase (Tables 2 and 3). The presence of palmitic, palmitoleic, stearic and linoleic acids indicated the stable formation of fatty acid composition (Table 3). The fatty acid profile differences between CC124 and sta6-1 were considered to be minor. In general, it was known that starchless mutant (sta6-1) accumulated higher content of lipid than wild type (CC124) under the nitrogen-depletion condition (Work et al., 2010; Siaut et al., 2011) but, in our work, sta6-1 mutant showed relatively a little increase in total lipid content (87.60 μg/ml) than wild type CC124 (85.60 μg/ml) at the late stationary phase (Table 3). The less difference of lipid content between mutant and wild type might be resulted from the cultivation in nitrogen-repletion condition (not in nitrogen-depletion condition as earlier report). In addition, our results demonstrating the fact that the mutants (sta6-1) do not show significantly high lipid content in nitrogen-repletion condition is a new observation.

3.5. Single cell sorting of C. reinhardtii

Using the single cell sort precision mode, individual Nile Red and BODIPY 505/515 stained CC124 and sta6-1 cells were separately sorted into 96-deep well plates containing 1 ml of TAP medium. Approximately ~79% of the cells (both CC124 and sta6-1) sorted with BODIPY 505/515 showed healthy growth (SI. F.6a). In order to determine the contamination rate in the sorted cells, 100 μl of the liquid portion from a randomly selected well was spread on a nitrogen-replete TAP agar plate and incubated for 7 days, and no bacterial and/or fungal contamination were observed (SI. F.6b and c). However, no cells sorted with Nile Red grew on TAP liquid medium (data not shown). BODIPY 505/515 stained single cells were sorted in combination with the concentrations of DMSO used in the study (0.02–0.2%), and no significant difference in their post-sorting viability and recovery was found between the different concentrations of DMSO used. By using a single cell sorting method and FACS screening, individual cells possessing high lipid content can be isolated successfully and used to seed new highly potent algal cultures. Post-sorting cell viability is mainly affected by toxic nature of dye and carrier substance used. It is also affected by fluid acceleration, electrical or mechanical shock, as well as by optical stress (Mutanda et al., 2011; Hyke et al., 2013). A study by Sinigalliano et al. (2009) compared the survival efficiency of fragile dinofagellate, Karenia brevis, between FACS sorting and manual picking. FACS sorting was shown to be less efficient than manual picking. This could be due to the fragility of algae that belong to this taxonomic group. Our initial effort was focused on determining the suitability of BODIPY and Nile Red for single cell sorting with appropriate solvents. Comparisons of post-sorting viability between BODIPY and Nile Red staining indicated that BODIPY in combination with DMSO was shown to be promising for single cell sorting. However, the rate of successful isolation of FACS sorted cells depends on fluorescent dye, carrier solvent, microalgal taxonomic group, and instruments used and require optimization of recovery conditions of microalgal culture.

3.6. The correlations between growth rates, cell sizes, FACS observations and FAME contents

The possibility of direct correlation between growth rates and cell sizes was also investigated by using FACS and FAME production. During the exponential phase (24–48 h), cell growth increased from 7.92×10^6 to 12.45×10^6 cells ml^{-1} (for CC124) and 10.95×10^6 to 23.92×10^6 cells ml^{-1} (for sta6-1) while cell size also increased (Table 1). FACS and fatty acid analysis showed the lipid accumulation was low in the exponential phase, but then constantly increased in the early-, and late-stationary phases (Table 2 and Table 3) and BODIPY 505/515 staining was positively correlated with fatty acid accumulation. It can be concluded that high cell growth and a limited lipid accumulation in the exponential phase are due to the production of proteins dominating (Doan et al., 2011). During the stationary phase, cell division was reduced due to a limitation of nutrients while accumulation of lipid content increased. In addition, the correlation coefficiency between Nile Red, BODIPY, and GC content was examined by using the samples

from exponential, early-, and late-stationary phases. In SI. F.7a–b, it is shown that the correlation coefficiency between Nile Red, BODIPY, and GC content was increased and fit well from exponential phase till late-stationary phase.

4. Conclusions

A high-throughput screening of *C. reinhardtii* using FACS in combination with BODIPY 505/515 labeling is described. BODIPY 505/515 in combination with a low concentration of DMSO can be effectively used for FACS screening, sorting and cell division of CC124 and its mutants. Importantly, both the flow cytometry BODIPY 505/515 staining and the physiological behavior results corresponded well with lipid accumulation in CC124 and sta6-1 cells. In conclusion, BODIPY 505/515 in combination with FACS should lead to the isolation of new algal strains possessing high lipid content and should lay a foundation for the single cell genomics study of microalgae for the production of advanced biofuels.

Acknowledgements

This work was supported by the Advanced Biomass R&D Center (ABC) of Korea Grant funded by the Ministry of Education, Science, and Technology (ABC-2010-0029728 and ABC-2012-053891). N. Velmurugan was supported by the BK21 Post-Doctoral Research Fund and Min S. Park was supported by the Brain Pool Program funded by the Korean Federation of Science and Technology Societies Grant by Korea Government (MEST, Basic Research Promotion Fund).

Appendix A. Supplementary data

Supplementary data associated with this article can be found, in the online version, at http://dx.doi.org/10.1016/j.biortech.2013.03.078.

References

Banerjee, A., Sharma, R., Chisti, Y., Banerjee, U.C., 2002. *Botryococcus braunii*: a renewable source of hydrocarbons and other chemicals. Crit. Rev. Biotechnol. 22, 245–279.

Beer, L.L., Boyd, E.S., Peters, J.W., Posewitz, M.C., 2009. Engineering algae for biohydrogen and biofuel production. Curr. Opin. Biotechnol. 20, 264–271.

Chen, W., Zhang, C., Song, L., Sommerfeld, M., Hu, Q., 2009. A high throughput Nile Red method for quantitative measurement of neutral lipids in microalgae. J. Microbiol. Methods 77, 41–47.

Chisti, Y., 2007. Biodiesel from microalgae. Biotechnol. Adv. 25, 294–306.

Cooksey, K.E., Guckert, J.B., Williams, S., Callis, P.R., 1987. Fluorometric dermination of the neutral lipid content of microalgal cells using Nile Red. J. Microbiol. Methods 6, 333–345.

Cooper, M.S., Hardin, W.R., Petersen, T.W., Cattolico, R.A., 2010. Visualizing "green oil" in live algal cells. J. Biosci. Bioeng. 109, 198–201.

Czechowska, M., Johnson, D.R., van der Meer, J.R., 2008. Use of flow cytometric methods for single-cell analysis in environmental microbiology. Curr. Opin. Microbiol. 11, 205–212.

Davey, H.M., Kell, D.B., 1996. Flow cytometry and cell sorting of heterogeneous microbial populations: the importance of single-cell analyses. Microbiol. Rev. 60, 641–696.

Doan, T.T.Y., Obbard, J.P., 2011a. Improved Nile Red staining of *Nannochloropsis* sp. J. Appl. Phycol. 23, 895–901.

Doan, T.T.Y., Obbard, J.P., 2011b. Enhanced lipid production in *Nannochloropsis* sp. using fluorescence-activated cell sorting. GCB Bioenerg. 3, 264–270.

Doan, T.T.Y., Sivaloganathan, B., Obbard, J.P., 2011. Screening of marine microalgae for biodiesel feedstock. Biomass Bioenergy 35, 2534–2544.

Folch, J., Lees, M., Stanley, G.H.S., 1957. A simple method for the isolation and purification of total lipids from animal tissues. J. Biol. Chem. 226, 497–509.

Goodson, C., Roth, R., Wang, Z.T., Goodenough, U., 2011. Structural correlates of cytoplasmic and chloroplast lipid body synthesis in *Chlamydomonas reinhardtii* and stimulation of lipid body production with acetate boost. Eukaryot. Cell 10, 1592–1606.

Gorman, D.S., Levine, R.P., 1966. Cytochrome f and plastocyanin: their sequence in the photosynthetic electron transport chain of *Chlamydomonas reinhardtii*. Proc. Natl. Acad. Sci. USA 54, 1669–1675.

Govender, T., Ramanna, L., Rawat, I., Bux, F., 2012. BODIPY staining, an alternative to the Nile Red fluorescence method for the evaluation intracellular lipids in microalgae. Bioresour. Technol. 114, 507–511.

Hyke, P., Lickova, S., Pribyl, P., Melzoch, K., Kovar, K., 2013. Flow cytometry for the development of biotechnological processes with microalgae. Biotechnol. Adv. 31, 2–16.

Li, Y., Han, D., Hu, G., Sommerfeld, M., Hu, Q., 2010. Inhibition of starch synthesis results in overproduction of lipids in *Chlamydomonas reinhardtii*. Biotechnol. Bioeng. 107, 258–268.

Merchant, S.S., 2007. The *Chlamydomonas* genome reveals the evolution of key animal and plant functions. Science 318, 245–250.

Mutanda, T., Ramesh, D., Karthikeyan, S., Kumari, S., Anandraj, A., Bux, F., 2011. Bioprospecting for hyper-lipid producing microalgal strains for sustainable biofuel production. Bioresour. Technol. 102, 57–70.

Pereira, H., Barreira, L., Mozes, A., Florindo, C., Polo, C., Duarte, C.V., Custodio, L., Varela, J., 2011. Microplate-based high throughput screening procedure for the isolation of lipid-rich marine microalgae. Biotechnol. Biofuels 4, 61–73.

Radakovits, R., Jinkers, R.E., Darzins, A., Posewityz, M.C., 2010. Genetic engineering of algae for enhanced biofuel production. Eukaryot. Cell 9, 486–501.

Siaut, M., Cuine, S., Cagnon, C., Fessler, B., Nguyen, M., Carrier, P., Beyly, A., Beisson, F., Triantaphylides, C., Li-Beisson, Y., Peltier, G., 2011. Oil accumulation in the model green alga *Chlamydomonas reinhardtii*: characterization, variability between common laboratory strains and relationship with starch reserves. BMC Biotechnol. 11, 7–22.

Sinigalliano, C.D., Winshell, J., Guerrero, M.A., Scorzetti, G., Fell, J.W., Eaton, R.W., Brand, L., Rein, K.S., 2009. Viable cell sorting of dinoflagellates by multiparametric flow cytometry. Phycologia 48, 249–257.

Wang, Z.T., Ullrich, N., Joo, S., Waffenschmidt, S., Goodenough, U., 2009. Algal lipid bodies: stress induction, purification, and biochemical characterization in wild-type and starch-less *Chlamydomonas reinhardtii*. Eukaryot. Cell 8, 1856–1868.

Williams, P.J.B., Laurens, L.M.L., 2010. Microalgae as biodiesel and biomass feedstocks: review and analysis of the biochemistry, energetics and economics. Energy Environ. Sci. 3, 554–590.

Work, V.H., Radakovits, R., Jinkerson, R.I., Meuser, J.E., Elliott, L.G., Vinyard, D.J., Laurens, L.M.L., Dismukes, G.C., Posewitz, M.C., 2010. Increased lipid accumulation in the *Chlamydomonas reinhardtii* sta7-10 starchless isoamylase mutant and increased carbohydrate synthesis in complemented strains. Eukaryot. Cell 9, 1251–1261.